

RANS Predictions of Turbulent Flow Past a Circular Cylinder over the Critical Regime

A. C. BENIM

Department of Mechanical and Process Engineering
Duesseldorf University of Applied Sciences
Josef-Gockeln-Str. 9, D-40474 Duesseldorf
GERMANY

M. CAGAN

Department of Mechanical and Process Engineering
Duesseldorf University of Applied Sciences
Josef-Gockeln-Str. 9, D-40474 Duesseldorf
GERMANY

A. NAHAVANDI

Department of Mechanical and Process Engineering
Duesseldorf University of Applied Sciences
Josef-Gockeln-Str. 9, D-40474 Duesseldorf
GERMANY

E. PASQUALOTTO

Development Engineer, Pelton Turbines
Andritz VA Tech Hydro AG
Hardstrasse 319, CH-8023 Zuerich
SWITZERLAND

Abstract: - Incompressible, turbulent flow past a circular cylinder is computationally investigated by means of Reynolds Averaged Numerical Simulations. Problems in using the wall-functions approach for modeling the near-wall turbulence are demonstrated. As the main turbulence model, the Shear Stress Transport model is employed, by resolving the near-wall layer. A wide range of Reynolds numbers is investigated ($Re=1 \cdot 10^4$ to $5 \cdot 10^6$), encompassing the critical regime. Predicted drag coefficients are compared with measurements from the literature. The procedure is shown to be able to predict the boundary layer transition and the associated drag coefficient reduction, qualitatively. Quantitatively, predicted drag coefficients are observed to underestimate measurements for all Reynolds numbers. Present analysis will be extended to more sophisticated transient models, which will be discussed in the oral presentation.

Key-Words: - Turbulent Flow Past Circular Cylinder, RANS, SST model, CFD.

1 Introduction

External flows around bluff bodies represents a very important area in fluid dynamics, with a large number of applications in many disciplines. Following the pioneering work of von Kármán [1], a very large and still rapidly growing body of literature has developed on the subject. Flows exhibiting particularly simple

configuration, such as flow past a circular cylinder or sphere have been subject of extensive experimental and computational investigation as the generic configurations. In the present analysis, a smooth and infinitely long cylinder blown by a unidirectional, homogeneous flow in unbounded domain is considered.

A number of computational investigations [2] analyzed the laminar flow at rather low Reynolds numbers (low-Re). The procedures for high Reynolds number (high-Re) flows include “no model” Large Eddy Simulations (LES) without using any explicit filter to set the scale of the dissipative mechanism [3], “pseudo” LES based on two-dimensional analysis [4] and Unsteady Reynolds Averaged Numerical Simulations (URANS) [5]. Steady-state, i.e. Reynolds Averaged Numerical Simulations (RANS) [6,7] were also performed. Allowed by improvements in computational capabilities, recent studies on the flow past a circular cylinder are increasingly based on the rather expensive procedures such as LES [8] and DES [9], which are surely capable of delivering more detailed and accurate results, compared to the simpler methods. However, if such sophisticated models shall really deliver more accurate results, they shall not be applied “straightforwardly”, but with some care [10]. This means that the grid shall be fine and the time step shall be small enough. These criteria become more severe with increasing Reynolds number. Thus, for large Reynolds numbers and complex geometries, as frequently encountered in industrial applications, they imply too high costs, even with today’s increased computational capabilities, for being applied as the state-of-the-art approach. Thus, there is still a need for applying less expensive approaches, for industrial purposes. The subject of the present paper is to perform a validation study for RANS modeling.

In Reynolds averaging, there are no explicit bounds on integration limits, and, the procedure, should, ideally/theoretically, represent an averaging over all time scales. But, the practice shows that a turbulence model applied within RANS can represent an averaging over the rather disorganized scales but not for the organized motion. There exists, but, no explicit control on such a scale separation in the models. The behavior of a certain model in a certain flow can only be assessed in application. In applying a RANS formulation to the present problem, it was, thus, expected that a part of the organized transient motion would not be represented by the turbulence model, and an inaccuracy would result. The quantification of the latter is a purpose of the present investigation.

Previous studies, which attempted to apply RANS procedures to the flow past a circular cylinder [6,7] used the $k-\varepsilon$ model [11] as the turbulence model, by applying additional empirical correlations for controlling the laminar-turbulent transition in the boundary layer. Such empirical correlations, however, may not easily be generalized to different flow situations and geometries and may be viewed to be of less significance for general applications. In the present study, the transition is not controlled by ad-hoc empirical criteria, but modeled directly by the applied RANS turbulence model, namely by the Shear Stress Transport (SST) model [12].

2 Modeling

Incompressible, turbulent flow of a Newtonian fluid is considered. Reynolds averaged Navier-Stokes and continuity equations are solved for two-dimensional, planar flow. At the inlet, a unidirectional flow and spatially constant variables are assumed. Inlet boundary conditions for turbulence quantities are derived by assuming a very low (0.01%) turbulence intensity and a turbulent-laminar viscosity ratio, implying, practically, a laminar flow. At the outlet, a zero gauge pressure is prescribed along with zero-gradient conditions for remaining variables. At walls, no-slip conditions apply. In addition to the above-mentioned boundaries, solution domains are enclosed by symmetry planes.

The computational analysis is performed using the general purpose CFD code Fluent 6.2 [13], which employs the finite volume method. For treating the velocity-pressure coupling, the SIMPLEC procedure [14] is employed. In the numerical discretization of the governing equations, a second order upwind scheme [15] is used for the convective terms. Solution domains are discretized by block-structured rectangular grids with conformal block interfaces. Grids are always generated based on grid independency studies. As the main turbulence model, the Shear Stress Transport (SST) model [12] is used in the present study. However, the $k-\varepsilon$ model [11] is also used in preliminary investigations. In the main computations, the wall layer is resolved, as the low-Re effects can be considered by the SST model. For application of the $k-\varepsilon$ model for resolving the wall layer (preliminary investigation), its two-layer-zonal amendment [16] is used for being able to consider low-Re effects. Computations are also performed using the wall-functions approach [11]. For a proper application of both strategies for the near-wall region, it is essential that the wall layer is adequately discretized. The important parameter in this context is the non-dimensional wall-distance y^+ of the next-to-wall cells, which is defined as $y^+ = (y/\nu)(\tau_w/\rho)^{0.5}$, where y , ν , τ_w and ρ denote the cell-to-wall distance, kinematic viscosity, wall shear stress, and density, respectively. If the wall layer is to be resolved by a low-Re model, the condition of $y^+ < 1$ shall be fulfilled. On the contrary, applying the wall-functions approach, y^+ shall be greater than 30 and preferably be in the range $100 > y^+ > 30$. Along with grid independency studies, grids are always generated by taking care for obtaining the most optimal y^+ values.

3 Preliminary Investigation

In a preliminary investigation, the ability of the available turbulence models to predict the natural transition is investigated. For this purpose, the boundary layer along a flat plate is analyzed. Here, the Reynolds number is typically defined as $Re_x = Ux/\nu$, where U , ν and x denote

the free stream velocity, kinematic viscosity, and coordinate direction in flow direction, respectively ($x=0$ at the leading edge). Length of the solution domain is defined so that $Re_x=1 \cdot 10^6$ is attained at the outlet. In y direction, domain extension is defined to be ten times larger than the maximum boundary layer thickness that is theoretically expected to occur [17] at the outlet. The rectangular solution domain is enclosed by a symmetry boundary on the top. Theoretically, it would be better to prescribe of a pressure boundary instead, which would allow mass transfer. But, this could not be done due to convergence difficulties. Nevertheless, disturbances associated with the symmetry boundary are expected to be negligible, since the lateral extension of the domain can be considered to be fairly large. Although, the wall-functions method is not expected to predict transition, it is still applied for demonstration purposes. Generated grids had an equidistant distribution in x direction with 1000 cells. In y direction, grid lines were concentrated near the wall, expanding into the domain by geometric expansion factors not larger than 1.2. This resulted in 30 cells for the grid to be used with the wall-functions and 80 cells for the grid resolving the wall layer.

In Fig. 1, predicted drag coefficients are compared with empirical/theoretical values [17] for laminar and turbulent boundary layer. One can see that the $k-\epsilon$ model with wall-functions ($k-\epsilon+WF$) performs poorly in initial parts of the boundary layer, and approaches empirical values for turbulent flow for large Re . The low- Re two-layer-zonal $k-\epsilon$ model ($k-\epsilon$), produces more reasonable values in initial, laminar parts of the boundary layer, but predicts a very early and weak transition at about $Re=10^4$. The SST model performs fairly well for low- Re . For $Re>10^4$, it shows a very good agreement with the laminar theoretical curve, and predicts a rather sharp transition to turbulence about $Re \approx 3-4 \cdot 10^5$ (theoretical value for transition: $Re = 5 \cdot 10^5$).

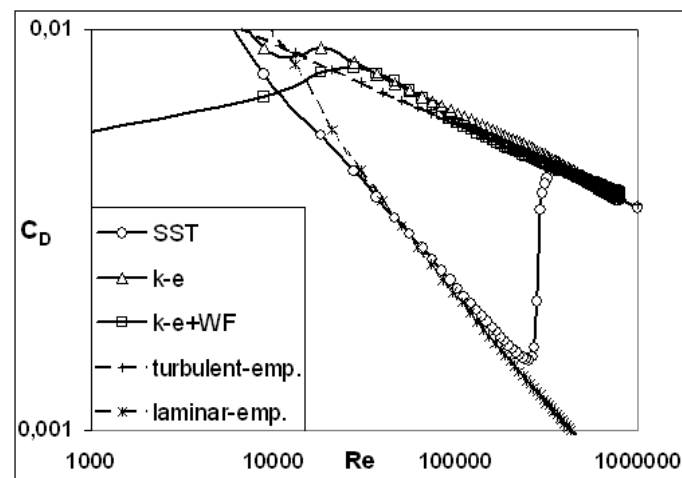


Fig. 1. C_D vs. Re for flat plate boundary layer.

4 Results

Based on the preliminary investigation, the SST model is used as the main turbulence model, in conjunction with wall-layer resolution. The solution domain and boundary types are shown in Fig. 2. Since the long time-averaged flow is symmetric, a symmetry plane is used, in the sense of RANS. Boundaries of the blocks used to generate the block-structured grid are also indicated in the figure. As one can see, the topology of the blocks implies principally an O-Type grid around the cylinder.

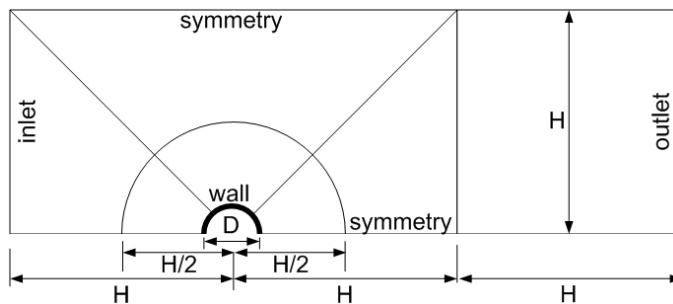


Fig. 2. Solution domain, boundaries, grid topology.

To find the optimal domain size, a domain size study is performed, by varying H (Fig. 2), for $Re=10^4$, using the SST model resolving the wall layer. Fig. 3 shows the variation of the predicted C_D with H . One can see that size influence is rather small beyond $H/D=6$. In the present computations, $H/D=10$ is used. In grid generation, as far as the resolution of the phenomena along cylinder surface is concerned, it was found that 100 cells for half cylinder circumference principally provide sufficient accuracy. (This number was about 80 in an LES analysis [8]). On the other hand, the condition $y^+ < 1$ requires a minimum cell height perpendicular to cylinder surface, which becomes smaller with increasing Re .

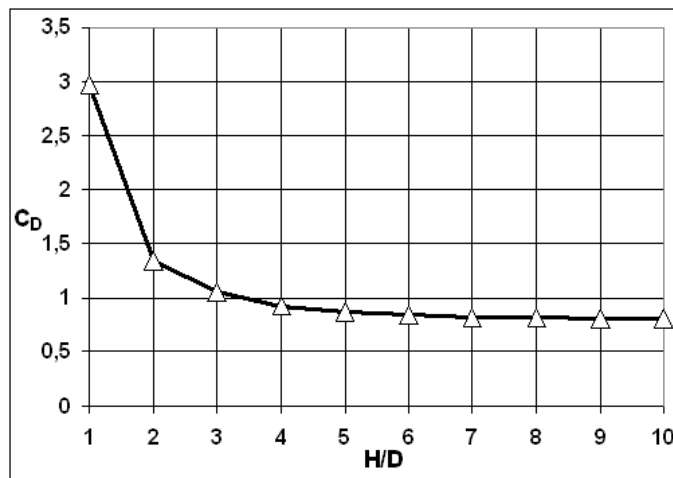


Fig. 3. C_D vs. H (SST, $Re=10^4$).

For the considered range of Re , this can lead to very strongly stretched cells. To relax the situation, 400 equidistantly distributed cells are used to discretize the half cylinder circumference, which allow four times smaller cell height, for the same aspect ratio, compared to 100 cells. For the cell height imposed by the $y^+ < 1$ condition, and using 400 equidistant cells along half cylinder circumference, a quite mild cell aspect ratio of 5 is obtained on the cylinder surface, for $Re=10^4$, which is the smallest Re considered. Away from the cylinder surface, the grid lines are geometrically expanded by rather mild expansion ratios (1.02 in the circular domain around the cylinder and 1.03-1.05 in the outer domain (Fig. 2)). The grid obtained for $Re=10^4$ this way had 92000 cells. Several further tests modifying the grid have shown that the results are grid independent. For larger Re , the $y^+ < 1$ condition implies always smaller cell heights, which would lead to larger aspect ratios, if the number of cells around the circumference are not increased. For decreasing the cell height to fulfill the $y^+ < 1$ condition with increasing Re , but keeping the same aspect ratio, without unnecessarily increasing the number of cells, the strategy of local grid refinement is

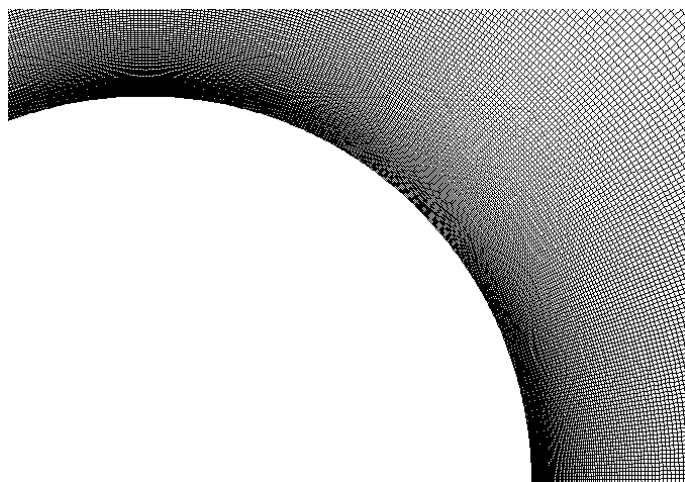


Fig. 4. Detail views of grids; above: $Re=10^4$, below: $Re=7 \cdot 10^5$.

used. Since the refinement is done non-conformally (hanging nodes), the grid outside the wall layer is not affected. Thus, the grid for $Re=10^4$ is used as the base grid for all cases. As Re is increased, the grid is refined as necessary to fulfill the $y^+ < 1$ condition for the considered Re . Fig. 4 shows detail views of the grids for $Re=10^4$, and $Re=7 \cdot 10^5$, where, local grid refinements can be seen. For $Re=5 \cdot 10^6$, seven refinement levels were necessary. Since the number of cells along cylinder circumference are also doubled by each refinement, this number became as large as 51200 for $Re=5 \cdot 10^6$. The total number of cells were 244000 for $Re=5 \cdot 10^6$, which is, but, not extremely large compared to 92000 cells of the base grid, due to the applied local grid refinement strategy. Since very small cells sizes result especially for high Re , all computations are performed using double precision.

Inadequacy of the wall-functions approach in predicting transition was already demonstrated. Another problem in using wall-functions in the present flow is that y^+ shows a continuous variation within a wide range. Therefore, it is difficult to attain favorable y^+ values throughout. Even if the mean value is in the favorable range ($100 > y^+ > 30$), local values may considerably vary. Additionally, the assumptions underlying the wall-functions approach are not necessarily valid in some important regions such as the vicinity of the separation point. Fig. 5 shows the drag coefficient values predicted by the $k-\epsilon$ model using wall-functions. Computations are performed using different grids, resulting in different “mean” y^+ values. In general, the grid is very fine. It is modified only in the vicinity of the cylinder wall, to obtain different y^+ values. In Fig. 5, C_D is shown as a function of the mean y^+ value. It is interesting to see that, there is no “plateau” for C_D values. It continuously changes with changing y^+ , including the favorable range ($100 > y^+ > 30$).

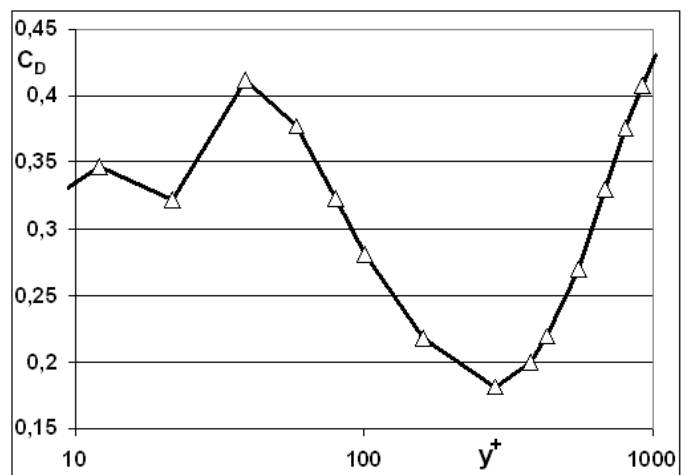


Fig. 5. C_D as function of average y^+ using wall-functions.

In other words, it does not seem to be possible to obtain “grid independent” results for the present problem at all, using the wall-functions.

Fig. 6 shows the variation of turbulent kinetic energy (k) along cylinder surface (position indicated by degrees (θ) from 0° to 180°) for $Re=10^5$ and $Re=5 \cdot 10^5$ obtained by the main turbulence model, i.e. SST model resolving the wall-layer (k values are nondimensionalized by the inlet turbulence kinetic energy (k_0)). These Re values can be considered to mark the borders of the critical regime, approximately. For $Re=10^5$, turbulence levels are rather low in the boundary layer. For $Re=5 \cdot 10^5$, a sharp increase occurs, followed by a decline.

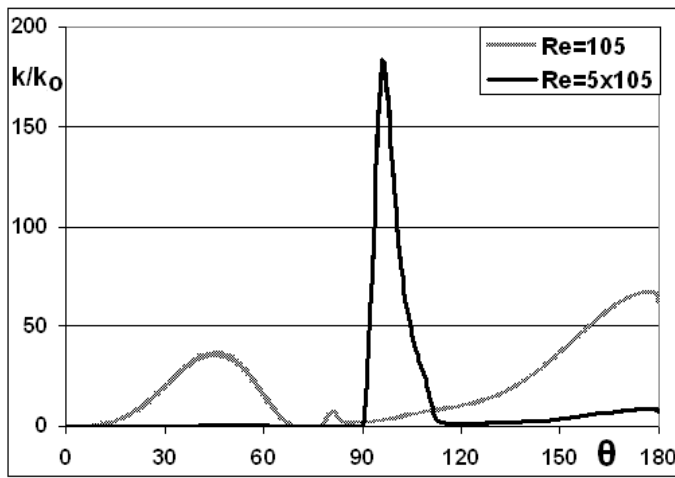


Fig. 6. Turbulence kinetic energy variation along cylinder surface for $Re=10^5$ and $Re=5 \cdot 10^5$.

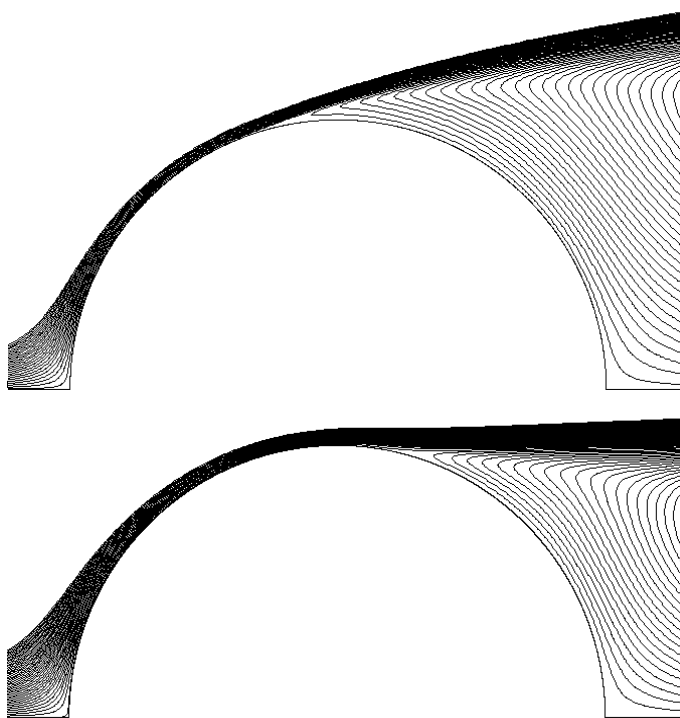


Fig. 7. Streamlines; above: $Re=10^5$, below: $Re=5 \cdot 10^5$.

The turbulence intensity and the region of high turbulence increase with further increasing the Reynolds number. Fig. 7. shows the streamlines in the near-field of the cylinder for both Re . One can clearly observe that the separation point moves further downstream with increasing Reynolds number from 10^5 to $5 \cdot 10^5$, and the recirculation zone became smaller.

Distribution of the static pressure along the cylinder surface for the same Reynolds numbers are shown in Fig 8. The reduction of the resultant pressure force for $Re=5 \cdot 10^5$ compared to $Re=10^5$, implying a corresponding reduction in the drag coefficient can be observed in the figure.

Predicted drag coefficients within the range from $Re=10^4$ to $Re=5 \cdot 10^6$ are presented in Fig. 9.

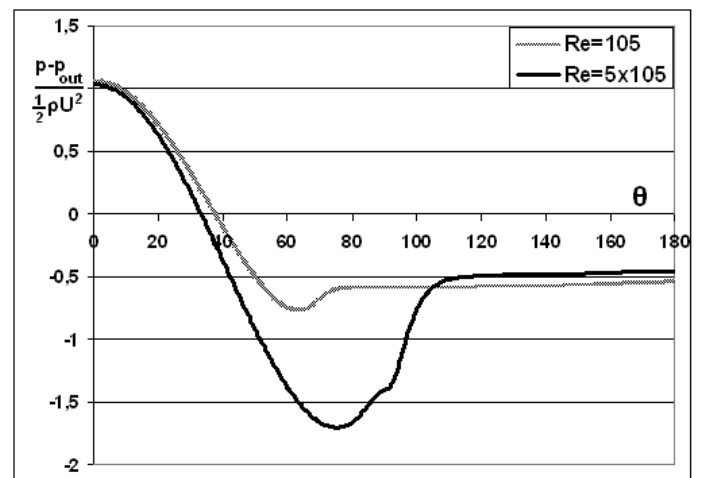


Fig. 8. Static pressure variation along cylinder surface.

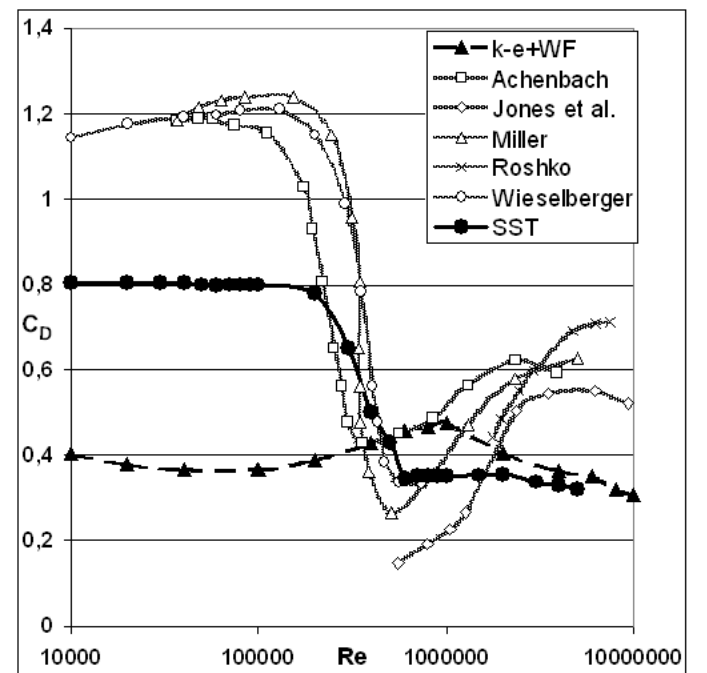


Fig. 9. C_D vs. Re : measurements [17] and predictions.

Besides the results obtained by the main turbulence model, i.e. the SST model by resolving the wall-layer, the $k-\epsilon$ model results obtained by the wall functions are also displayed for comparison ($k-\epsilon$ +WF). Measured values obtained by different authors (borrowed from a compilation by Bohl and Elmendorf [17]) are also shown in the figure. It is interesting to note that the measurements also show variations within a rather broad range, depending on the particular experimental conditions. One can see that the computations using the wall-functions do not predict any transition, as expected. The variations in the drag coefficients predicted by the wall-functions may be caused by the strong grid dependency of C_D i.e. strong dependency of C_D on y^+ demonstrated above (Fig. 5), although a quite optimal mean value for y^+ was obtained in each case. One can see that the main turbulence model, i.e. the SST model resolving the wall layer can qualitatively predict the reduction of the drag coefficient over the critical regime. Quantitatively, predicted drag coefficients are observed to underestimate measurements for all Reynolds numbers. This is apparently due to the contribution of the organized transient motion, which could not be modeled by the present RANS approach.

5 Conclusion

Turbulent flow past a circular cylinder is investigated by means of a RANS formulation. Problems in using the wall-function approach for modeling the near-wall turbulence are discussed. As the main turbulence model, the SST model is used in combination with a grid resolving the near-wall layer. A wide range of Reynolds numbers (10^4 - $5 \cdot 10^6$) encompassing the critical regime is analyzed. It is shown that the boundary layer transition and the associated drag coefficient reduction can qualitatively be predicted by the SST model resolving the boundary layer. Quantitatively, the predicted drag coefficients underestimate the measurements throughout. This is expected to be due to the influence of the organized transient motion, which could not be taken into account by the RANS-SST formulation. Based on the present results, the analysis is intended to be extended towards the more sophisticated approaches including transient, three-dimensional procedures such as LES.

References:

- [1] von Kármán, Th., "Über den Mechanismus des Widerstandes, den ein bewegter Körper in einer Flüssigkeit erzeugt", *Nachr. Ges. Wiss. Göttingen, Math. Phys. Klasse*, 1911, pp. 509-517.
- [2] Braza, M., Chassaing, P. and Ha Minh, H., "Numerical study and physical analysis of the pressure and velocity fields in the near wake of a circular cylinder", *J. Fluid Mech.*, Vol.165, 1986, pp. 79-130.
- [3] Tamura, T., Ohta, I. and Kuwahara, K., "On the reliability of two-dimensional simulation for unsteady flows around a cylinder-type structure", *Journal of Wind Engineering and Industrial Aerodynamics*, Vol. 35, 1990, pp. 275-298.
- [4] Song, C. C. S. and Yuan, M., "Simulation of vortex shedding flow about a circular cylinder at high Reynolds numbers", *ASME Journal of Fluids Engineering*, Vol. 112, 1989, pp. 155-163.
- [5] Franke, R., "Numerische Berechnung der instationären Wirbelablösung hinter zylindrischen Körpern" Ph. D. Dissertation, Department of Civil Engineering, Univ. Karlsruhe, Germany, 1991.
- [6] Majumdar, S. and Rodi, W., "Numerical calculation of turbulent flow past circular cylinders", *Proceedings of the Third Symposium on Physical Aspects of Aerodynamic Flows* Long Beach, California, 21-24 January, 1985.
- [7] Celik, I. and Shaffer, F. D., "Long time-averaged solutions of turbulent flow past a circular cylinder", *Journal of Wind Engineering and Industrial Aerodynamics*, Vol. 56, 1995, 185-212.
- [8] Franke, J. and Frank, W., "Large eddy simulation of the flow past a circular cylinder at $Re_D=3900$ ", *Journal of Wind Engineering and Industrial Aerodynamics*, Vol. 90, 2002, pp. 1191-1206.
- [9] Strelets, M., "Detached eddy simulation of massively separated flows", *AIAA 2001-0879*, 2001.
- [10] Fröhlich, J., Mellen, C. P., Rodi, W., Temmerman, L. and Leschziner, M. A., "Highly resolved large-eddy simulation of separated flow in a channel with streamwise periodic constrictions", *Journal of Fluid Mechanics*, Vol. 526, 2005, pp. 19-66.
- [11] Launder, B. E. and Spalding, D. B., "The numerical computation of turbulent flows", *Comput. Meths. Appl. Mech. Engng.*, Vol. 3, 1974, pp. 269-289.
- [12] Menter, F. R., "Two equation eddy-viscosity turbulence models for engineering applications", *AIAA Journal*, Vol. 32, 1994, pp. 1598-1695.
- [13] *Fluent 6.2, User's Guide* (Fluent Inc., 2006).
- [14] Vandoormal, J. P. and Raithby, G. D., "Enhancements of the SIMPLE method for predicting incompressible flows", *Numerical Heat Transfer*, Vol. 7, 1984, pp. 147-163.
- [15] Barth, T. J. and Jespersen, D., "The design and application of upwind schemes on unstructured meshes", *AIAA-89-0366*, 1989.
- [16] Wolfstein, M., "The velocity and temperature distribution of one-dimensional flow with turbulence augmentation and pressure gradient", *International Journal of Heat and Mass Transfer*, Vol. 12, 1969, pp 301-318.
- [17] Bohl, W. and Elmendorf, W., *Technische Strömungslehre*, 13. Ed. (Vogel, Würzburg, 2005).